Microstructures and Shape Memory Effect of Different Carbon-Bearing FeMnSiCrNi Alloys Aged after Equal Channel Angular Pressing

WEI ZHANG, NING LI, and YUHUA WEN

The microstructures and shape memory effect in FeMnSiCrNi0.02C and FeMnSiCrNi0.12C fabricated to equal channel angular pressing (ECAP) and subsequent aging were studied. The results reveal that after ECAP and subsequent aging, the optimal shape recovery ratio of FeMnSiCrNi0.12C aged after ECAP is 89.4 pct, 20 pct higher than FeMnSiCrNi0.02C. Microstructural analysis shows that many carbide precipitates in FeMnSiCrNi0.12C aged after ECAP effectively suppress grain coarsening. As a result, FeMnSiCrNi0.12C obtains a better shape memory effect than FeMnSiCrNi0.02C due to the finer grains together with second-phase hardening by carbide precipitation.

DOI: 10.1007/s11663-007-9022-9

I. INTRODUCTION

THE Fe-Mn-Si-Cr-Ni shape memory alloys not only exhibit good machinability, good workability, and good weldability, but also good corrosion resistance. However, the poor shape memory effect (SME) limits their application. To improve the SME, various factors, including the sorts and contents of alloying element[1,2,3] annealing treatment,[4] precipitation of second phase,[5,6] and thermomechanical training,[6–8] have been investigated. So far, the thermomechanical training is the most effective method to improve the SME. However, this kind of treatment is difficult for practical application because of its complexity of treating processes.

The SME in Fe-Mn-Si-Cr-Ni shape memory alloys results from the stress-induced $\gamma \rightarrow \varepsilon$ martensite transformation and its reversion. Accordingly, increasing the strength of the matrix and decreasing the critical stress for stress-induced martensite transformation can both suppress the intrusion of permanent slip and thus improve the SME. Grain refinement is an effective way to strengthen the matrix. Sato[9] found that the average size of grains in thin foil specimens fabricated by rapid quenching was about 1.5 to 5.0 μm, and the shape memory effect was 90 pct when bent by 4 pct at 77 K. However, the technique of rapid quenching cannot produce bulk alloys.

In our previous work,[10] it was revealed that in an FeMnSiCrNi alloy fabricated by equal channel angular pressing (ECAP) and subsequent annealing, fine grains were produced and thus the SME was improved to some extent. In fact, the ECAP technology, introduced by Segal,[11] has been successfully applied to produce various ultra-fine-grained materials, such as Al alloys,[12] low carbon steels,[13] and Mg alloys.[14] However, to eliminate the great numbers of dislocations and shearing bands, annealing after ECAP is inevitable, which will lead to the coarsening of grains. For example, in pure Al, Al-Mg alloys, and Al-Zr alloys fabricated by ECAP,[15] the grain size grows from submicrometer annealed at 300 K to 100 μm when being annealed at 600 K. Similarly, the grains of low carbon steel grow from 0.5 to 20 μm when the annealing temperature is increased from 400 to 1073 K.[16]

Some research revealed that strain-induced NbC precipitations could effectively suppress the grains' coarsening during annealing in the hot-rolling Nb microalloyed steels.[17,18] Therefore, in the present work, ECAP was used to refine the grains and, in the meantime, precipitation of carbides was applied to suppress the grain coarsening. This article compared the microstructures and SME of two kinds of alloys bearing different carbon contents. The results revealed that after ECAP and subsequent aging at 973 K, in alloy II (FeMnSiCrNi0.12C), many carbides were produced and the grains were finer; a shape recovery ratio of 89.4 pct was obtained when the prestrain was 4.33 pct, 20 pct higher than alloy I (FeMnSiCrNi0.02C) aged after ECAP. A finer grain together with second-phase hardening by $Cr_{23}C_6$ carbides was the main reason for the better SME in alloy II.

II. EXPERIMENTAL PROCEDURES

The experimental alloys were prepared by induction furnace melting under argon atmosphere, using high-purity iron, manganese, silicon, chromium, nickel, and graphite. After being homogenized at 1373 K for 15 hours, the cylindrical ingots with a diameter of 80 mm and a height of 140 mm were first hot forged to rods with a diameter of 15 mm and length of 100 mm.

WEI ZHANG, Postdoctoral Candidate, NING LI and YUHUA WEN, Professors, are with the College of Manufacturing Science and Engineering, Sichuan University, Chengdu 610065, People's Republic of China. Contact e-mail: zwatt@163.com

Manuscript submitted May 22, 2006.
Article published online March 29, 2007.

The rods were annealed at 1373 K for 30 minutes, again to eliminate the as-forged microstructures, followed by water quenching. Some of the as-quenched rods were machined to rods with a diameter of 12 mm to experience the process of ECAP. The chemical compositions of the alloys were determined by SPECTROLAB direct-reading spectrograph as follows (in mass pct):

Alloy I: 18.95Mn, 4.96Si, 8.55Cr, 4.63Ni, 0.02C, and balance Fe.
Alloy II: 19.04Mn, 4.98Si, 8.50Cr, 4.59Ni, 0.12C, and balance Fe.

Figure 1 demonstrates schematically the die of ECAP. The diameter of the channel in the die is 12.4 mm, and the internal angle Φ is 120 deg. First, the rod coated by graphite lamella was put in the channel; then, the die and rod were heated to 573 K and held for 20 minutes; finally, the rod was pressed through the die with a speed of 1 mm/s. According to Reference 19, the microstructural evolution occurred most rapidly if the rod was rotated through 90 deg between the repetitive pressings. Therefore, the rod was rotated by 90 deg about the longitudinal axis and again put in the channel and held at 573 K for 20 minutes, and then pressed through the die with the same speed. The specimens were subjected to two passages of ECAP.

To measure the SME, the wires with a diameter of 1.3 mm and length of 100 mm were cut from the as-pressed rods and as-quenched rods using a Mo filament cutter, respectively. The wires were cut parallel to the longitudinal axis of the rod. Both the as-pressed and as-quenched specimens of alloy I and alloy II were aged at 573 to 1073 K for 150 minutes. The shape recovery ratio η was tested by the traditional bending method, as described in Reference 4. The predeformation temperature is 293 K and the specimens were heated to 673 K for recovery. The martensite phase transformation temperature (*Ms*) was determined by the electric resistivity-temperature curves.

The microstructures were determined using a JSM-5900LV scanning electron microscope. As-pressed specimens for transmission electron microscope (TEM) were jet polished with a 20 pct sulfuric acid and 80 pct methanol solution and observed by a TECNAI F20 electron microscope operating at 200 kV. The second phase was characterized by an X'Pert Pro MPD X-ray diffraction (XRD) instrument.

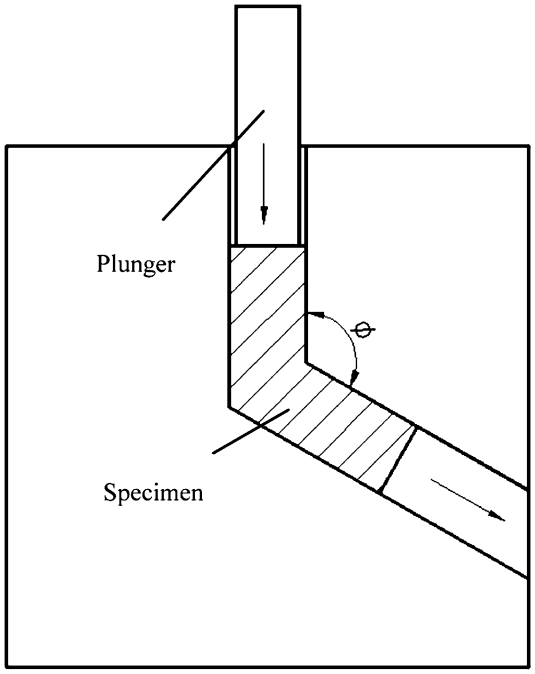

Fig. 1—Schematic illustration of ECAP.

III. RESULTS AND DISCUSSION

A. *Effects of Aging Temperature*

Figure 2 shows the effects of aging temperature on the shape recovery ratio η of alloy I and alloy II, respectively. Aging had little effect on the η of the as-quenched alloy I. After being pressed, when the aged temperature was low, the η of alloy I was much lower, and with an increase in the aged temperature, η increased fast and reached the maximum value of 74 pct at 973 K, and then decreased with the further increasing aged temperature. For alloy II aged without pressing, η increased with the increasing aging temperature and reached the maximum value of 65 pct at 973 K. After being pressed, the trend of η *vs* aging temperature of alloy II was similar to alloy I being pressed. However, the maximum value of η was 89.4 pct, 20 pct higher than that of alloy I, which was aged after ECAP.

Table I shows the martensite phase transformation temperature (*Ms*) of alloy I and alloy II subjected to different treatments. First, the addition of carbon remarkably decreased the *Ms* temperature of alloy II. Next, the *Ms* temperature of both alloy I and alloy II decreased due to the grain refinement after ECAP and

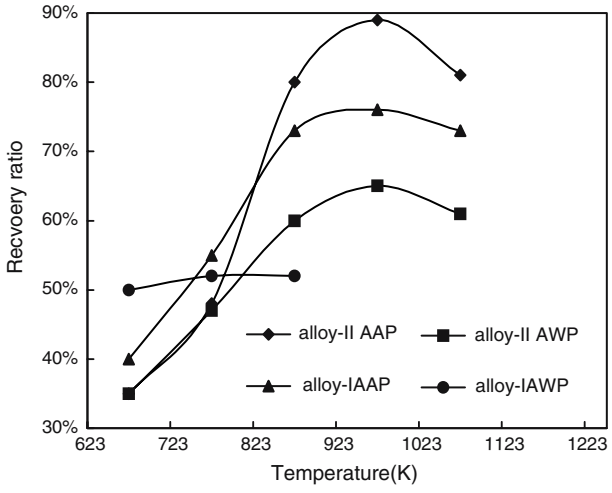

Fig. 2—Effects of aging temperature (for 150 min) on the shape memory ratio of alloys aged after pressing (AAP) and aged without pressing (AWP) (ε = 4.33 pct).

Table I. *Ms* Temperatures of Alloy I and Alloy II Aged at 973 K for 30 Minutes after ECAP and without ECAP

	As-Quenched	Aging without Pressing	Aging after Pressing
Ms (K) of alloy I	263	—	240
Ms (K) of alloy II	225	247	228

aging. However, after being aged, carbide precipitation increased the *Ms* temperature of both the as-quenched and as-pressed alloy II.

B. *Microstructures of the Alloys after ECAP and Aging*

Figure 3 is the SEM micrograph of alloy I and alloy II aged at 973 K without pressing. The average size of the grains of alloy I was about 150 μm, and there was no second phase in alloy I aged at 973 K for 150 minutes. In fact, the microstructures of as-quenched alloy I, as-aged alloy I, and as-quenched alloy II were similar, as in Figure 3(a). For alloy II aged at 973 K, some second phases were precipitated and mainly at grain boundaries. The average size of the grains was also about 150 μm.

Figure 4 is a TEM micrograph of specimens subjected to ECAP. After pressing, the grain boundary was poorly defined and high-density dislocations were introduced.

Figure 5 is the SEM micrograph of (a) alloy I and (b) alloy II, both aged at 973 K for 150 minutes after ECAP. The recrystallizations in alloy I and alloy II were completed. In alloy I, the average size of grains was about 20 μm and there were no carbides. In the meantime, some grains coarsened. For alloy II aged at 973 K after ECAP, the size of grains was more uniform than that of alloy I and the average size of the grains was about 10 μm. In the meantime, there were great numbers of tiny second phase distributed in grains and at grain boundaries.

The XRD analysis in Figure 6 determined that precipitation in specimens aged without pressing (Figure 3(b)) and those being aged after pressing (Figure 5(b)) were both $Cr_{23}C_6$. Furthermore, the amount of $Cr_{23}C_6$ in alloy II being aged after pressing was much more than that in those aged without pressing.

The SME in Fe-Mn-Si-Cr-Ni alloys is the result of the stress-induced ε-martensite transformation and its reverse transformation. Therefore, to obtain a good SME, a shape change must be accomplished by the stress-induced ε-martensite transformation, avoiding the occurrence of permanent slip. Research[7–10] confirms that grain refinement and carbide precipitate hardening could both improve the strength of Fe-Mn-Si-based alloys, thus improving the SME.

The ECAP is one of the effective methods of introducing intense plastic straining and thus strength to the matrix. However, when the ageing temperature is too low, many dislocations remain and thus block the slip of Shockley partial dislocations. Consequently, to induce martensite transformation, a higher drive energy is required and the *Ms* temperature is obviously decreased, resulting in a low SME. With increasing aging temperature, the density of dislocations decreases and as-pressed structures begin to recover; thus, the slip of the Shockley partial dislocations becomes easy and the SME increases. After being aged at 973 K, the average size of recrystallized grains in both alloy I and alloy II after ECAP is remarkably finer than those without ECAP. According to the Hall–Petch formula,[20,21]:

$$\sigma = \sigma_0 + Kd^{-1/2},$$

where σ_0 and K are constant, d is the average size of the grain, and σ is the strength of the matrix. The

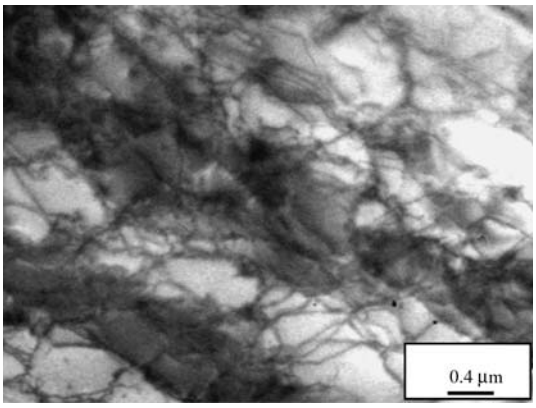

Fig. 4—TEM micrographs of alloy II subjected to ECAP.

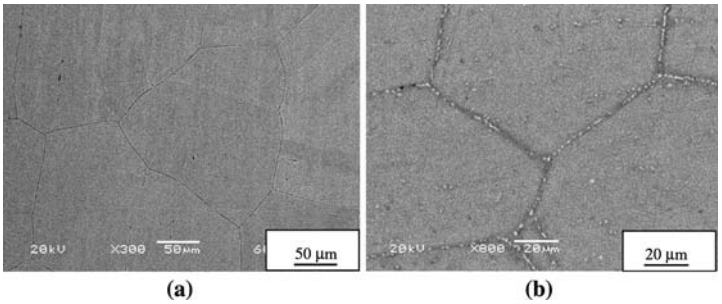

Fig. 3—SEM micrographs of (a) alloy I and (b) alloy II aged at 973 K for 150 min without pressing.

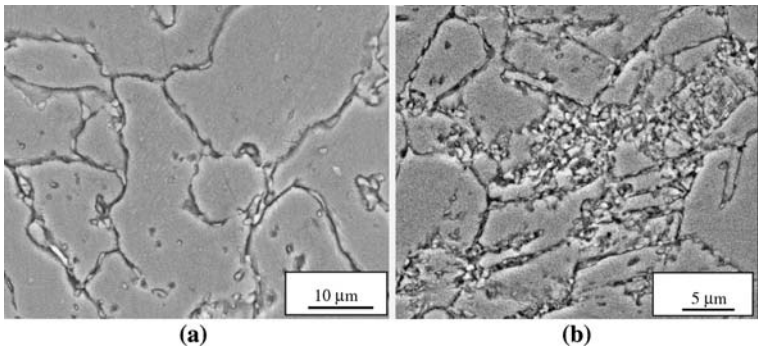

Fig. 5—SEM micrographs of the average size and carbide precipitations in as-pressed (a) alloy I and (b) alloy II aged at 973 K for 150 min.

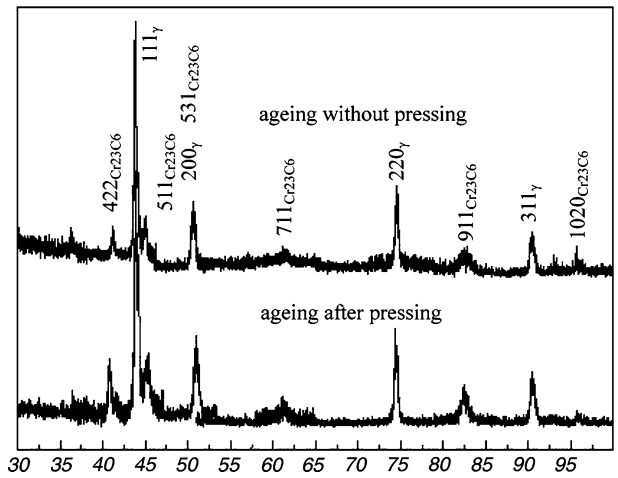

Fig. 6—XRD analysis of the as-pressed specimens aged at 873 K for 150 min.

strength of the austenite matrix should be remarkably increased. According to Sato's research, grain refinement can block the slip of dislocation and thus enable more strain to be afforded by stress-induced $\gamma \rightarrow \varepsilon$ phase transformation. Meantime, the cross of stress-induced ε martensite plates with different variants is decreased in fine grains.[9]

However, after aging to eliminate the dislocations introduced by ECAP, the grain coarsening occurs in alloy I, which decreases the strengthening of the matrix by refinement. The present work suggests that precipitate of second phase can effectively inhibit the grains coarsening during aging. The reason is that, after ECAP, there exist a high-density dislocation area and shearing bands. These dislocations can remarkably decrease the activation energy for precipitate nucleation.[22] As a result, more carbides are introduced in alloy II aged after ECAP before the recrystallization is completed. Consequently, these carbides effectively impede the grains' coarsening.

In fact, these carbides can also strengthen the austenite matrix of the specimens, inhibiting the plastic. In the meantime, precipitation of carbides increases the *Ms* temperature. As a result, aging has little effect on η of alloy I, but η of alloy II being aged without pressing increases to some extent with the increasing aging temperature. For alloy II being aged after pressing, the amount of the carbides is much greater and the strength of the austenite matrix is further increased. Consequently, although the decreasing *Ms* temperature was a disadvantage to SME, alloy II being aged after pressing obtains a better SME due to the carbide precipitations together with its suppression of grain coarsening. In fact, other factors such as the content of carbides, the amount and size of the carbides, and the strain induced by ECAP can also affect the shape memory behavior in addition to the parameters studied. The results of this study are based on only two alloys and a wider and more systematic study is required to validate the findings.

IV. CONCLUSIONS

After ECAP and subsequent aging, the optimal shape recovery ratio of the FeMnSiCrNi0.12C is 89.4 pct, 20 pct higher than that of FeMnSiCrNi0.02C aged after ECAP and 40 pct higher than that of FeMnSiCrNi0.12C aged without ECAP. First, ECAP can refine the grains of two alloys and improve their SME. On the other hand, during aging after ECAP, more carbide precipitations are introduced in FeMnSiCrNi0.12C. These carbide precipitations effectively suppress the grain coarsening and in the meantime strengthen the matrix. As a result, FeMnSiCrNi0.12C obtains a better shape memory effect than FeMnSiCrNi0.02C due to the finer grains together with second-phase hardening by carbide precipitation.

ACKNOWLEDGMENTS

The work was supported by the National Natural Science Foundation of China (Grant No. 50501015) and the Ph.D. Programs Foundation of the Ministry of Education of China (Grant No. 20030610093).

REFERENCES

1. A. Sato, E. Chishima, K. Soma, and T. Mori: *Acta Metall*., 1982, vol. 30, pp. 1177–83.
2. A. Sato, Y. Yamaji, and T. Mori: *Acta Metall*., 1986, vol. 34, pp. 287–94.
3. H. Otsuka, H. Yamada, T. Maruyama, T. Mori, H. Tanahashi, S. Matsuda, and M. Murakami: *ISIJ Int*., 1990, vol. 30, pp. 674–79.
4. B.C. Maji and M. Krishnan: *Scripta Mater*., 2003, vol. 48, pp. 71–77.
5. S. Kajiwara, D. Liu, T. Kikuchi, and N. Shinya: *Scripta Mater*., 2001, vol. 44, pp. 2809–14.
6. A. Baruj, T. Kikuchi, S. Kajiwara, and N. Shinya: *Mater. Sci. Eng. A*, 2004, vol. 378, pp. 333–36.
7. C.Y. Chung, C. Shuchuan, and TY. Hsu: *Mater. Characterization*, 1996, vol. 37, pp. 227–36.
8. N. Bergeon, S. Kajiwara, and T. Kikuchi: *Acta Metall*., 2000, vol. 48, pp. 4053–64.
9. A. Sato, T. Masuya, M. Morishita, S. Kumai, and A. Inoue: *Mater. Sci. Forum*, 2000, vols. 327–328, pp. 223–26.
10. Y.H. Wen, M. Yan, and N. Li: *Scripta Mater*., 2004, vol. 50, pp. 441–44.
11. V.M. Segal: *Mater. Sci. Eng. A*, 1995, vol. 197, pp. 157–64.
12. J.R. Bowen, O.V. Mishin, P.B. Prangnell, and D.J. Jansen: *Scripta Mater*., 2002, vol. 47, pp. 289–94.
13. H.K. Kim, M. Choi, C.S. Chung, and D.H. Shin: *Mater. Sci. Eng. A*, 2003, vol. 340, pp. 243–50.
14. H.K. Lin, J.C. Huang, and T.G. Langdon: *Mater. Sci. Eng. A*, 2005, vol. 402, pp. 250–57.
15. H. Hasegawa, S. Komura, and A. Utsunomiy: *Mater. Sci. Eng. A*, 1999, vol. 265, pp. 188–96.
16. D.H. Shin, B.C. Kim, and K.T. Park: *Acta Mater*., 2000, vol. 48, pp. 3245–52.
17. F.J. Humphreys: *Acta Mater*., 1997, vol. 45, pp. 5031–39.
18. X.Y. Song, N.J. Gu, and G.Q. Liu: *Acta Metall. Sinica*, 2000, vol. 36, pp. 592–96.
19. Y. Iwahashi, M. Furukawa, Z. Horita, M. Nemoto, and T.G. Langdon: *Mater. Sci. Eng. A*, 1998, vol. 257, pp. 328–32.
20. E.O. Hall: *Proc. Phys. Soc., London*, 1951, vol. 64B, pp. 747–53.
21. N.J. Petch: *J. Iron Steel Inst*., 1953, vol. 174, pp. 25–28.
22. B. Dutta, E.J. Palmiere, and C.M. Sellars: *Acta Mater*., 2001, vol. 49, pp. 785–94.